The Polar Nature of 7-Ketocholesterol Determines Its Location within Membrane Domains and the Kinetics of Membrane Microsolubilization by Apolipoprotein A-I†

John B. Massey* and Henry J. Pownall

Section of Atherosclerosis and Lipoprotein Research, Department of Medicine, Baylor College of Medicine, One Baylor Plaza, Houston, Texas 77030

Received April 6, 2005; Revised Manuscript Received May 27, 2005

ABSTRACT: 7-Ketocholesterol is an oxidized derivative of cholesterol with numerous physiological effects. In model membranes, 7-ketocholesterol and cholesterol were compared by physical measures of bilayer order and polarity, formation of detergent resistant domains (DRM), phase separation, and membrane microsolubilization by apolipoprotein A-I. In binary mixtures of a saturated phosphatidylcholine (PC), dipalmitoyl-PC (DPPC), and cholesterol or 7-ketocholesterol, the sterols modulate bilayer order and polarity and induce DRM formation to a similar extent. Cholesterol induces formation of ordered lipid domains (rafts) in tertiary mixtures with dioleoyl-PC (DOPC) and DPPC, or DOPC and sphingomyelin (SM). In tertiary mixtures, cholesterol increased lipid order and reduces bilayer polarity more than 7-ketocholesterol. This effect was more pronounced when the mixtures were in a miscible liquid-disordered (L_d) phase. Substitution of 7-ketocholesterol for cholesterol dramatically reduced the extent of DRM formation in DOPC/DPPC and DOPC/SM bilayers and ordered lipid phase separation in mixtures of a spin-labeled PC with DPPC and with SM. Compared to cholesterol, 7-ketocholesterol decreased the rate for the microsolubilization of dimyristoyl-PC multilamellar vesicles by apolipoprotein A-I. The membrane effects of 7-ketocholesterol were dependent on the phospholipid matrix. In L_d phase phospholipids, a model for 7-ketocholesterol indicates that the proximity of the 7-keto and 3β-OH groups puts both polar moieties at the lipid−water interface to tilt the sterol nucleus to the plane of the bilayer. 7-Ketocholesterol was less effective in forming ordered lipid domains, in decreasing the level of bilayer hydration, and in forming phase boundary bilayer defects. Compared to cholesterol, 7-ketocholesterol can differentially modulate membrane properties involved in protein−membrane association and function.

Oxidized derivatives of cholesterol, oxysterols, are important structural and biologically active lipid components located within cell membranes. They may be important regulators of the biophysical properties of the plasma membrane microdomains termed lipid rafts (*1*−*6*). 7-Ketocholesterol is a major cytotoxin of oxidized LDL[1] (*7*−*9*). In macrophage foam cells isolated from atherosclerotic lesions, oxysterols were 6−9% of the total sterol concentration where 50% was 7-ketocholesterol (*10*). In cultured cells with 7-ketocholesterol levels similar to that in lesion macrophage foam cells, free 7-ketocholesterol is located primarily within Triton X-100 detergent resistant membranes (*5*, *6*, *11*). DRMs isolated from these cholesterol-loaded macrophages contain ∼60% sphingolipids, and 7-ketocholesterol represents 35% of the total sterol concentration (*5*). This amount of membrane sterol may be required for the in vitro cell biological effects of 7-ketocholesterol. The 7-ketocholesterol in plasma membrane rafts may be mechanistically linked to altered signal transduction (*6*, *11*) and DRM protein composition (*6*), and inhibition of apoA-I-mediated cholesterol efflux (*5*). The molecular basis of the cellular effects of 7-ketocholesterol is currently unknown.

Oxysterols are involved in the normal regulation of cholesterol homeostasis and in the pathogenesis of atherosclerosis (*7*−*9*, *12*−*14*). 7-Ketocholesterol, the major oxysterol in oxidized LDL and atherosclerotic lesions (*10*, *15*), modulates many cellular processes, possibly through effects within the plasma membrane (*5*, *6*). In humans, 7-ketocholesterol is formed primarily by the nonenzymatic oxidation of cholesterol (*13*). Reverse cholesterol transport, which involves the efflux of cholesterol from peripheral tissue where it is synthesized to the liver for recycling or degradation, is an important cardioprotective mechanism. Efflux of cholesterol from the plasma membrane to apolipoproteins

† Supported by grants from the National Institutes of Health (HL-30914 and HL-56865 to H.J.P.).

* To whom correspondence should be addressed: Section of Atherosclerosis and Lipoprotein Research, Department of Medicine, Baylor College of Medicine, The Methodist Hospital, MS A-601, 6565 Fannin St., Houston, TX 77030. Phone: (713) 798-4141. Fax: (713) 798-4121. E-mail: jbm@bcm.tmc.edu.

[1] Abbreviations: ABCA1, ATP-binding cassette transporter A-1; apoA-I, apolipoprotein A-I, the major protein component of human high-density lipoproteins; DMPC, dimyristoyl-*sn*-glycero-3-phosphocholine; DOPC, dioleoyl-*sn*-glycero-3-phosphocholine; DPH, 1,6-diphenyl-1,3,5-hexatriene; DPPC, dipalmitoyl-*sn*-glycero-3-phosphocholine; DRM, detergent-resistant membranes; GP, generalized polarization; HDL, high-density lipoproteins; Laurdan, 6-dodecanoyl-2-dimethylaminonaphthalene; L_o, liquid-ordered phase; L_d, liquid-disordered phase; LDL, low-density lipoproteins; MLV, multilamellar vesicles; POPC, 1-palmitoyl-2-oleoyl-*sn*-glycero-3-phosphocholine; SUV, small unilamellar vesicles; 12SLPC, 1-palmitoyl-2-stearoyl-(12-doxyl)-*sn*-glycero-3-phosphocholine; rHDL, reassembled HDL; RCT, reverse cholesterol transport; SM, sphingomyelin; T_M, midpoint temperature of the gel to liquid-crystalline phase transition.

10.1021/bi0506425 CCC: $30.25
Published on Web 07/09/2005

and high-density lipoproteins initiates RCT, and within the context of cardioprotection, oxysterols regulate cholesterol efflux (*5*, *16*−*19*), scavenger receptor BI (*20*) and apoE gene expression (*21*), and intracellular cholesterol movement (*22*). ApoA-I triggers cholesterol efflux through the ABCA1 pathway (*5*, *16*, *23*), and its inhibition may be a direct effect of 7-ketocholesterol on interactions of apoA-I with the plasma membrane (*5*, *16*). However, 7-ketocholesterol may also directly inhibit the lipid transporter activity of ABCA1 or affect a substrate pool of cholesterol. 7-Ketocholesterol also modulates intracellular communication (*24*) and calcium-mediated signal transduction (*6*, *25*), and the induction of monocyte differentiation (*26*), apoptosis (*9*, *14*, *27*−*30*), and LDL oxidation (*31*). Some of these effects may be due to intracellular binding proteins, although a protein with high affinity and specificity for this oxysterol has not been identified (*32*). Oxysterols may alter the lipid and protein composition and the biophysical properties of lipid rafts that may be mechanistically linked to their many diverse pathological effects (*5*, *6*).

The condensing−ordering effects of oxysterols are rate when compared to those of cholesterol (*4*, *33*−*36*). For example, in DPPC/DOPC bilayers, 7-ketocholesterol was not as effective as cholesterol in stabilizing ordered lipid domains (*4*). Although the behavior of 7-ketocholesterol simulates that of cholesterol, its effects on the interfacial region of the bilayer that includes the phosphate and the acyl ester groups are more profound, suggesting that hydration of the 7-keto group anchors the sterol to the interfacial region (*3*, *35*, *37*, *38*). The carbonyl group of 6-ketocholestanol, which is a sterol structurally similar to 7-ketocholesterol, affects the membrane dipole potential which can alter such processes as peptide−membrane association (*39*). One measure of lipid polarity and the affinity between sterols and phospholipids is the rate of spontaneous transfer between membranes (*40*). 7-Ketocholesterol transfers ~20 times faster than cholesterol from DPPC SUV, whereas the more polar 7α-hydroxycholesterol and 7β-hydroxycholesterol were more than 100 and 200 times faster, respectively (*41*). The structural modulation of membrane microdomains by oxysterols may be an important determinant of their biology. However, the partitioning of oxysterols between different lipid phases and their effects on membrane structure remain to be defined. The interaction of apoA-I with the ABCA1 transporter on the plasma membrane initiates cholesterol effux, the first step in RCT. This initial step in apoA-I lipidation is a function of membrane structure in vitro (*42*−*44*) and likely in vivo (*5*, *16*, *45*−*47*). Thus, we conducted studies that would establish a mechanistic link between the effects of 7-ketocholesterol and cholesterol on membrane properties and the interaction of membranes with apoA-I.

EXPERIMENTAL PROCEDURES

Materials. 7-Ketocholesterol was from Steraloids, Inc. (Newport, RI). DMPC, DPPC, DOPC, POPC, 12SLPC, and brain SM were from Avanti Polar Lipids, Inc. (Alabaster, AL). Laurdan and DPH were from Molecular Probes, Inc. (Eugene, OR). High-purity cholesterol was from Calbiochem-Novabiochem (La Jolla, CA). Human plasma apoA-I was isolated as described previously (*48*).

Liposome Preparation. Phospholipids, sterols, and fluorescent probes were combined in a chloroform/methanol mixture (2/1, v/v), which was removed under a nitrogen stream after which the residue was dried overnight under vacuum. The dried lipids were dispersed in TBS [100 mM NaCl, 10 mM Tris, 1 mM EDTA, and 1 mM NaN_3 (pH 7.4)] by vortexing. The lipids were subjected to three freeze−thaw cycles of warming to 50 °C, which exceeds the thermal phase transition of the highest melting lipids, and freezing to −20 °C. The mixed phospholipid systems had DOPC/DPPC (1/1 molar ratio) and DOPC/SM (3/2 molar ratio) compositions. For the fluorescence studies, the probe-to-phospholipid molar ratio was 1/250.

Fluorescence Measurements. Fluorescence measurements were performed on a Jobin Yvon (Edison, NJ) Spex Fluorolog-3 FL3-22 spectrofluorimeter, which was equipped with Glan-Thompson polarizing prisms and a sample heater/cooler Peltier thermocouple drive. Fluorescence polarization measurements were performed as previously described (*49*). The fluorescence polarization of DPH, which partitions equally into gel, liquid-crystalline, and liquid-ordered phases (*50*), was used to measure the effect of sterol structure on the acyl chain motion and phase properties of phospholipid bilayers in MLVs (*51*). The excitation and emission wavelengths were 350 and 430 nm, respectively. The polarization was corrected for the grating factor.

The fluorescence measurements with the polarity sensitive probe, Laurdan, were collected with an excitation wavelength of 350 nm; fluorescence intensity measurements were taken at 430 and 480 nm. The ratio of fluorescence intensities at 430 (I_{430}) and 480 nm (I_{480}) were used to calculate the generalized polarization of Laurdan [$GP = (I_{430} - I_{480})/(I_{430} + I_{480})$] (*51*, *52*). Like DPH, this probe partitions equally between gel and liquid-crystalline phases. Temperature-dependent measurements for DPH and Laurdan were collected in 1 °C increments; the samples were equilibrated for 1 min prior to each measurement. When required, temperature profiles were fitted to a sigmoidal regression analysis (Sigma Plot 8.0) from which the midpoint temperature (T_M) marking a 50% change in the fluorescence value was calculated according to the relation $p(T) = p_0 + a/\{1 + \exp[-(T - T_M)/b]\}$, where $p(T)$ is the measured fluorescence value at temperature T and p_0, a, b, and T_M are constants (*51*).

The fluorescence quenching assay of London et al. (*1*, *2*, *4*, *50*) was used to measure the effect of 7-ketocholesterol on domain formation. Liposomes containing 12SLPC and DPPC (1/1 molar ratio) and 12SLPC and SM (3/2 molar ratio) with 0.5 mol % DPH were prepared. Samples contained either no sterol or 15 mol % sterol composed of various ratios of cholesterol and 7-ketocholesterol. Fluorescence spectra were recorded between 380 and 550 nm with excitation at 350 nm. The data were expressed as the fluorescence increase which was the ratio of peak fluorescence intensity (I_{429}) of samples with 15 mol % sterol to those without sterol.

DRM Formation. Phospholipids and sterols that form tightly packed, L_o domains resist solubilization by Triton X-100 (*1*, *4*, *50*, *53*, *54*). Solubilization was assessed by a previously described procedure (*1*, *4*, *50*). The initial turbidity of MLVs (500 nmol of phospholipid in 1 mL of TBS) was measured on a Cary 25 spectrophotometer as the optical density at 400 nm (OD_{400}). A 50 μL portion of 10% (w/v) Triton X-100 in TBS was added to each of the samples after which the samples were mixed and incubated at room

temperature overnight, and OD_{400} was determined. The solubilization (ΔOD_{400}) was determined as the ratio of OD_{400} after the Triton X-100 incubation (not corrected for dilution with Triton X-100 solution) to that measured before the addition of Triton X-100.

Kinetics of the Solubilization of DMPC Multilamellar Vesicles by ApoA-I. The rate of solubilization of multilamellar vesicles of DMPC containing various amounts of sterol by apoA-I was determined by measuring the time-dependent decrease in liposomal turbidity (*42*−*44*, *48*). The principle of this method is that large multilamellar DMPC vesicles (diameter of >10000 Å) are turbid and scatter light, whereas after the addition of apoA-I is the formation of small rHDL (diameter of ∼100 Å) which are transparent. The change in turbidly can be used to estimate the rate of rHDL formation. MLVs (0.5 mg of phospholipids) were preincubated at various temperatures and mixed with apoA-I (0.25 mg) in a final volume of 3 mL in a fluorescence cuvette. Clearance of turbidity was followed as the reduction in right-angle light scattering measured in the fluorimeter using excitation and emission wavelengths of 325 nm. The sample was continuously stirred to prevent the MLVs from settling out of solution. The data were analyzed as a first-order kinetic process using Sigma-Plot statistical software. The rHDL so formed were characterized by nondenaturing polyacrylamide gel electrophoresis on 4 to 20% gradient gels (Bio-Rad Laboratories, Hercules, CA).

RESULTS

Fluorescence Studies of Phase Behavior. In DMPC and DPPC MLVs, the DPH fluorescence polarization decreases sharply at the respective gel to the L_d phase transition temperatures ($T_M \sim 23.1$ °C for DMPC and $T_M \sim 40.6$ °C for DPPC) (*55*). Cholesterol and 7-ketocholesterol (15 mol %) demonstrate essentially identical behavior in modulating the phase transitions where acyl chain order was decreased (i.e., lower polarization) below T_M and increased (i.e., higher polarization) above T_M (Figure 1A,B). There was a difference between the phospholipid bilayers where the modulation in DMPC was mainly reduced above T_M. Both sterols increased GP below and above T_M (Figure 2A,B) and modulated changes in GP associated with T_M. This effect was similar to that reported for cholesterol/SM bilayers (*51*). Increased GP values have been assigned to closer lipid packing that decreases membrane polarity and the level of hydration of the interfacial region (*51*, *52*).

In DOPC/SM MLVs, DPH fluorescence polarization shows no phase transition and the polarization values are consistent with a miscible L_d phase between 25 and 55 °C (*56*, *57*) (Figure 1C). The increased fluorescence polarization with the addition of 15 mol % cholesterol or 7-ketocholesterol indicates increased acyl chain order. Over the same temperature range, the fluorescence polarization of DPH in DOPC/DPPC bilayers revealed a broad phase transition at ∼35−40 °C that was indicative of solid−liquid immiscibility below ∼35 °C (Figure 1D) (*57*, *58*). Addition of either sterol eliminated the phase transition and increased the polarization of DPH fluorescence, with the ordering effect of cholesterol being greater than that of 7-ketocholesterol.

Cholesterol dramatically increased the GP in DOPC/SM and DOPC/DPPC MLVs (Figure 2C,D). GP was higher with

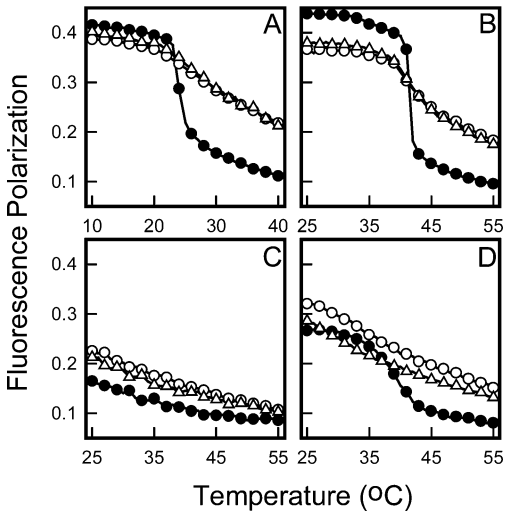

FIGURE 1: Effect of cholesterol and 7-ketocholesterol on the fluorescence polarization of DPH in DMPC (A), DPPC (B), DOPC/SM (3/2 molar ratio) (C), and DOPC/DPPC (1/1 molar ratio) (D) bilayers measured as a function of temperature. The measurements are for bilayers than contain no added sterol (●), 15 mol % cholesterol (○), and 15 mol % 7-ketocholesterol (△). The phospholipid concentration was 0.1 mg/mL, and the probe/phospholipid molar ratio was 1/250.

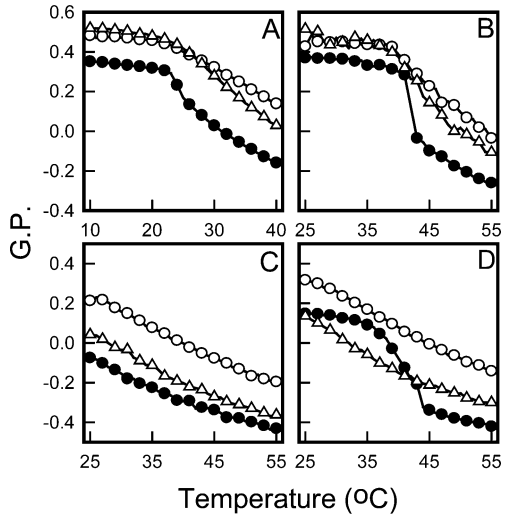

FIGURE 2: Effect of cholesterol and 7-ketocholesterol on the generalized polarization (GP) of Laurdan in DMPC (A), DPPC (B), DOPC/SM (3/2 molar ratio) (C), and DOPC/DPPC (1/1 molar ratio) (D) bilayers measured as a function of temperature. The measurements are for bilayers than contain no added sterol (●), 15 mol % cholesterol (○), and 15 mol % 7-ketocholesterol (△). The phospholipid concentration was 0.1 mg/mL, and the probe/phospholipid molar ratio was 1/250.

the addition of cholesterol than with 7-ketocholesterol. Consistent with the measurements of DPH fluorescence polarization in DOPC/DPPC bilayers, cholesterol and 7-ketocholesterol inhibit fluid phase−gel phase immiscibility below ∼35 °C (Figure 2D). The modulating effects of 7-ketocholesterol and cholesterol on DPH fluorescence polarization in DOPC/SM and DOPC/DPPC MLVs were similar; however, the effects of 7-ketocholesterol on GP were smaller than those of cholesterol.

Dose Effects of Sterol Concentration on Model Membranes. The effects of sterol concentration on DPH fluorescence polarization and GP in DPPC bilayers were dose-dependent above (55 °C; L_d phase) and below (25 °C; L_o

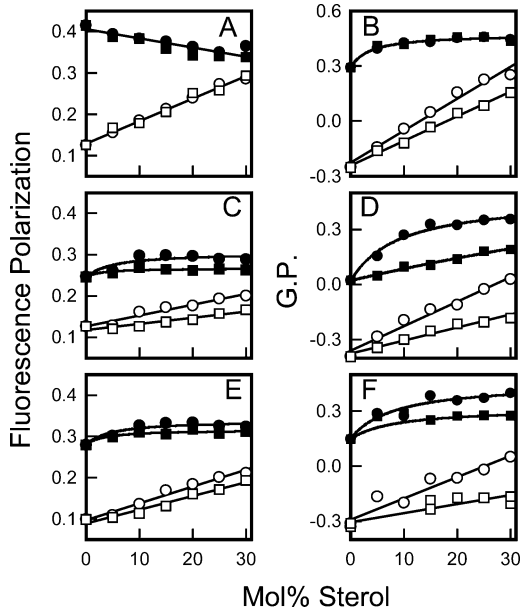

FIGURE 3: Fluorescence polarization of DPH (A, C, and E) and the generalized polarization of Laurdan (B, D, and F) measured in DPPC (A and B), DOPC/SM (3/2 molar ratio) (C and D), and DOPC/DPPC (1/1 molar ratio) (E and F) bilayers as a function of sterol concentration. The phospholipid bilayers contained cholesterol (● and ○) and 7-ketocholesterol (■ and □), and the fluorescence measurements were taken at 25 °C (● and ■) and 55 °C (○ and □).

phase) its T_M. At 55 and 25 °C, the DPH fluorescence polarization increased and decreased linearly, respectively, with the sterol concentration with the effects of cholesterol and 7-ketocholesterol being indistinguishable (Figure 3A). The effects of the two sterols on GP in DPPC were more distinctive (Figure 3B). At 55 °C, the GP increased linearly with both sterols with the slope being higher for cholesterol than for 7-ketocholesterol. At 25 °C, the dose effects of the sterols on the GP were identical with a slight increase at low sterol concentrations that was nearly constant between 5 and 30 mol %.

L_o and L_d phases coexist at 25 °C in cholesterol-containing DOPC/DPPC and DOPC/SM MLVs (*56*−*59*). At 25 °C, the dose effects of the sterols on the DPH fluorescence polarization in DOPC/SM and DOPC/DPPC bilayers were similar with a slight increase at low sterol concentrations and little change between 5 and 30 mol % (Figure 3C,E). The effects on GP were similar except for the linear response observed for 7-ketocholesterol in DOPC/SM bilayers. Cholesterol increased the fluorescence values more than 7-ketocholesterol did.

At 55 °C, which is above the T_M of DOPC, DPPC, and SM, the bilayers are in a L_d phase, even in the presence of sterol (*56*−*59*). This temperature is above the miscibility transition temperature for the mixed bilayers. In both DOPC/DPPC and DOPC/SM bilayers, the fluorescence polarization and GP increased linearly with sterol concentration. Comparison of the slopes (ΔP/mol % and ΔGP/mol %) (Table 1) revealed that cholesterol altered the membrane properties more than 7-ketocholesterol. For the GP measurements, the ratios of the slopes ($\Delta GP_{KC}/\Delta GP_C$) were 0.75, 0.53, and 0.42 for DPPC, DOPC/SM, and DOPC/DPPC bilayers, respectively.

Effect of the Cholesterol/7-Ketocholesterol Ratio on Lipid Order. The effects of substituting 7-ketocholesterol for cholesterol at a constant total sterol concentration (15 mol %) on DPH fluorescence polarization and GP were determined to test whether the reported synergistic effect of 7-ketocholesterol and cholesterol on the properties of DPPC bilayers in the L_d phase (*35*) might extend to more complex lipid mixtures (Figure 4). Positive and negative synergism would present as curves above and below a line connecting 0 and 100 mol % 7-ketocholesterol, respectively; in the absence of synergism, a straight line would connect 0 and 100 mol %. According to these criteria, none of the lipid mixtures exhibited synergism with respect to the effects of 7-ketocholesterol and cholesterol on DPH fluorescence polarization and GP. A straight line, corresponding to no synergism, was found, suggesting that each sterol contributed to DPH fluorescence polarization and GP in an amount that was proportional to its mole percent in the mixture. This was observed for phospholipids above their T_M (DOPC, POPC, and DMPC) and below their T_M (DPPC) and for mixtures with coexisting L_o and L_d phases (DOPC/DPPC and DOPC/SM). It is notable that as the number of saturated acyl chains in a PC decreases (DPPC, POPC, and DOPC), the DPH fluorescence polarization and GP decrease at all ratios of cholesterol and 7-ketocholesterol.

Effect of Sterols on Lipid Solubility in Triton X-100. The formation of DRMs was assessed in different phospholipid MLVs as a function of the 7-ketocholesterol/cholesterol ratio at a constant total sterol content (15 mol %; Figure 5). In the presence of sterol, the level of DRM formation was highest for DPPC followed by mixtures of DOPC with DPPC and SM, and DMPC with little or no DRM formation by DOPC and POPC. According to ΔOD_{400}, there was some DRM formation by DMPC bilayers with cholesterol, an effect that was eliminated by replacing cholesterol with 7-ketocholesterol. There was no DRM formation in POPC or DOPC MLVs with either sterol. Although DRMs were formed by cholesterol-containing DOPC/DPPC and DOPC/SM MLVs, the level of DRM formation decreased linearly to ∼45 and ∼90%, respectively, when cholesterol was replaced with an increasing fraction of 7-ketocholesterol. The results for DPPC, DOPC, and DOPC/DPPC MLVs containing 15 mol % cholesterol or 7-ketocholesterol are similar to those of Wang et al. who used a higher concentration of sterol (25 mol %) (*4*).

Fluorescence Quenching Assay for Domain Formation. The effects of sterol on the collisional quenching of DPH fluorescence in 12SLPC/DPPC and 12SLPC/SM liposomes were measured. DPH fluorescence in sterol-free bilayers is highly quenched because the phospholipids form miscible L_d phases. The addition of either sterol greatly reduces the 12SLPC-mediated fluorescence quenching which reflects the formation of a coexisting L_o phase from which 12SLPC is excluded, whereas DPH is distributed equally into L_d and L_o phases (*1*, *2*, *4*). Thus, the increase in fluorescence intensity with the added sterol is due to separation of lipids into an L_d phase containing 12SLPC where DPH fluorescence is quenched and a sterol-rich/SM or sterol-rich/DPPC L_o phase from which 12SLPC is excluded and there is no fluorescence quenching, with the magnitude of the fluorescence increase reflecting the amount of lipid converted to the L_o phase.

Table 1: Comparison of the Slopes (ΔP/mol % and ΔGP/mol %) for the Effect of Cholesterol and 7-Ketocholesterol on the Properties of L_d Phase DPPC, DOPC/SM, and DOPC/DPPC Bilayers at 55 °C

phospholipid	sterol	ΔP/mol % $\times 10^3$	$\Delta P_{KC}/\Delta P_C$[a]	ΔGP/mol % $\times 10^2$	$\Delta GP_{KC}/\Delta GP_C$
DPPC	cholesterol	5.48	0.99	1.75	0.75
	7-ketocholesterol	5.41		1.34	
DOPC/SM	cholesterol	2.62	0.56	1.33	0.53
	7-ketocholesterol	1.49		0.71	
DOPC/DPPC	cholesterol	4.06	0.82	1.16	0.42
	7-ketocholesterol	3.33		0.49	

[a] Ratio of the slopes ($\Delta P_K/\Delta P_C$ and $\Delta GP_K/\Delta GP_C$) for bilayers containing cholesterol (C) and 7-ketocholesterol (KC).

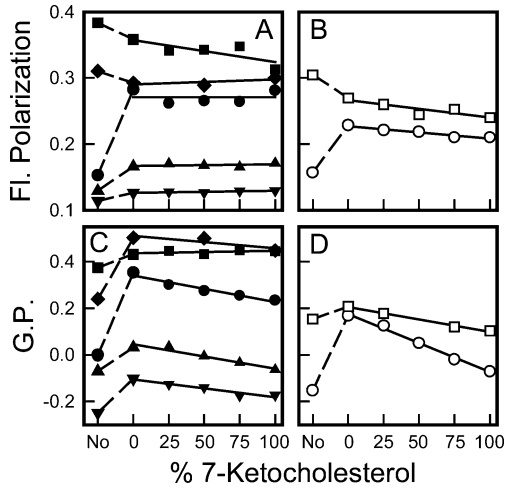

FIGURE 4: Fluorescence polarization of DPH (A and B) and the generalized polarization of Laurdan (C and D) were assessed in phospholipid bilayers in which the cholesterol/7-ketocholesterol ratio was varied but the total sterol content (15 mol % sterol) was kept constant. The cholesterol/7-ketocholesterol ratio is expressed as the percentage of 7-ketocholesterol as calculated from the equation % 7-ketocholesterol = (moles of 7-ketocholesterol)/(moles of cholesterol + moles of 7-ketocholesterol) × 100. The bilayers contained DMPC (●), DPPC (■), POPC (▲), DOPC (▼), and SM (◆) in panels A and C and DOPC and SM (3/2 molar ratio) (○) and DOPC and DPPC (1/1 molar ratio) (□) in panels B and D. The GP and DPH polarization measurements were also performed on phospholipid bilayers that contained no (No) additional sterol. The temperature for these measurements was 30 °C.

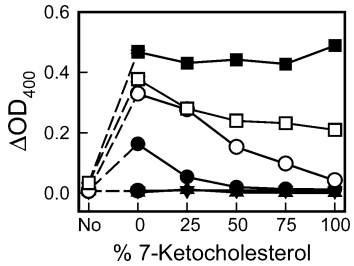

FIGURE 5: Extent of solubilization of phospholipid bilayers measured as ΔOD_{400} which was the ratio of the OD measured at 400 nm with and without Triton X-100. The bilayers contained DMPC (●), DPPC (■), POPC (▲), DOPC (▼), DOPC and SM (3/2 molar ratio) (○), and DOPC and DPPC (1/1 molar ratio) (□). In the different phospholipid bilayers, the cholesterol/7-ketocholesterol ratio was varied but the total sterol content (15 mol % sterol) was kept constant. The cholesterol/7-ketocholesterol ratio is expressed as the percentage of 7-ketocholesterol as calculated from the equation % 7-ketocholesterol = (moles of 7-ketocholesterol)/(moles of cholesterol + moles of 7-ketocholesterol) × 100. The samples were incubated overnight at room temperature ($T \sim 23$ °C). Each sample was measured in triplicate and is represented as the mean (symbol) ± the standard error (error bars).

At 25 °C, the respective incorporation of 15 mol % cholesterol and 7-ketocholesterol into 12SLPC/SM bilayers increased the DPH fluorescence intensity 4.6- and 1.6-fold, respectively (Figure 6A). These increases reflect formation of L_o domains, more of which are induced by cholesterol than by 7-ketocholesterol. Comparison of DPPC and SM bilayers indicated that the addition of cholesterol to both bilayers increased fluorescence; however, the increase was much greater in 12SLPC/DPPC bilayers (Figure 6B), suggesting more DPPC than SM was converted to the L_o phase. However, substituting increasing amounts of 7-ketocholesterol for cholesterol decreased the fluorescence intensity (increased quenching) in 12SLPC/SM bilayers, while there was a small increase in intensity in 12SLPC/DPPC bilayers. Thus, substitution of 7-ketocholesterol for cholesterol reduced the fraction of 12SLPC/SM in the L_o phase but only slightly increased the fraction of lipid in the L_o phase in 12SLPC/DPPC bilayers.

At 37 °C, DPH fluorescence intensity in 12SLPC/DPPC bilayers containing 15 mol % cholesterol was higher than that in 12SLPC/SM bilayers, and the substitution of increasing amounts of 7-ketocholesterol for cholesterol decreased DPH fluorescence intensity (increased quenching) in both DPPC and SM. Thus, at 37 °C, sterols induce more L_o domains in DPPC liposomes than in those of SM, and substitution of 7-ketocholesterol for cholesterol produces a linear decrease in the amount of lipid in the L_o phase with both SM and DPPC (Figure 6C). Using an identical method, Wang et al. (*4*) observed that 20 mol % 7-ketocholesterol was as effective as 20 mol % cholesterol in forming DPPC-rich L_o domains in 12SLPC/DPPC mixtures over the temperature range of 25−55 °C. We observe different temperature dependences between the two sterols (15 mol %) in 12SLPC/DPPC mixtures at 25 and 37 °C. In 12SLPC/SM bilayers, the two sterols behave very differently.

Lipid−Protein Interactions: Kinetics of Solubilization of DMPC Liposomes by ApoA-I. ApoA-I spontaneously associates with DMPC multilamellar vesicles which results in their solubilization to form rHDL with a defined structure and stoichiometry (*42*, *43*). The effects of 10 mol % cholesterol and 7-ketocholesterol on the kinetics of this process were measured below (22.8 °C), at (24.2 °C), and above (26.2 °C) the T_M of DMPC. Solubilization of sterol-free liposomes above and below T_M was very slow, but the rate increased dramatically at the transition temperature where gel and L_d phases coexist (Table 2) (*42*, *43*). The addition of either sterol to form a coexisting L_o phase increased the rate, where a greater increase in the rate was observed for cholesterol than for 7-ketocholesterol at all three temperatures (Figure 7A−C). Below, at, and above T_M, 10 mol % cholesterol increased the rate 160-, 2.3-, and 9.7-fold, respectively, when compared

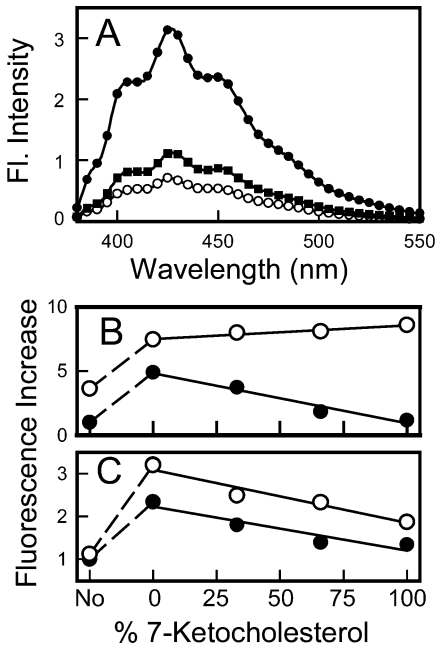

FIGURE 6: Sterol-induced formation of lipid domains as assessed by fluorescence quenching of DPH (0.5 mol %) in liposomes of 12SLPC and DPPC (1/1 molar ratio) or 12SLPC and SM (3/2 molar ratio) at 25 °C. In panel A, fluorescence spectra of DPH in 12SLPC/SM (3/2 molar ratio) liposomes containing no sterol (○), 15 mol % cholesterol (●), and 15 mol % 7-ketocholesterol (■) demonstrate that the fluorescence intensity was dependent on the sterol structure and the sterol concentration. The increase in fluorescence intensity in the presence of cholesterol was indicative of the formation of phase-separated membrane domains. In panels B and C, a fluorescence increase was calculated as the ratio of the fluorescence intensity measured at 429 nm for a given sample to that of 12SLPC/SM (3/2 molar ratio) liposomes containing no sterol. In 12SLPC/DPPC (1/1 molar ratio) (○) and 12SLPC/SM (3/2 molar ratio) (●) bilayers, the cholesterol to 7-ketocholesterol ratio was varied but the total sterol content (15 mol % sterol) was kept constant. The samples were measured at 25 (B) and 37 °C (C). The cholesterol/7-ketocholesterol ratio is expressed as the percentage of 7-ketocholesterol as calculated from the equation % 7-ketocholesterol = (moles of 7-ketocholesterol)/(moles of cholesterol + moles of 7-ketocholesterol) × 100. The samples were at a phospholipid concentration of 150 μM.

to the rate with DMPC alone, and 7-ketocholesterol increased the rate 100-, 1.6-, and 3.6-fold, respectively (Table 2). The rate of solubilization of DMPC increased linearly between 0 and 10 mol % sterol (Figure 8A), and at all sterol concentrations, the cholesterol-induced enhancement of apoA-I solubilization was greater than that of 7-ketocholesterol. At a higher sterol content (>15 mol %), the rate is slower (data not shown). At a constant total sterol concentration (10 mol %), the rate of solubilization of DMPC by apoA-I decreased linearly with an increasing 7-ketocholesterol/cholesterol ratio, an effect observed below, at, and above T_M (Figure 8B).

According to nondenaturing gradient gel electrophoresis, the rHDL formed with and without 5 mol % cholesterol and 7-ketocholesterol was a single product with a diameter of ~100 Å (Figure 9). The major products formed with DMPC containing 10 mol % cholesterol or 7-ketocholesterol had a diameter of ~170 Å. Similar rHDL products were formed by various ratios of cholesterol and 7-ketocholeserol when the total sterol concentration is kept constant (data not shown).

DISCUSSION

Cholesterol is a major lipid component of cell membranes and plasma lipoproteins. Under normal physiological conditions, oxysterols are minor lipid components that are formed enzymatically and are involved in cholesterol homeostasis and catabolism. However, toxic oxysterols such as 7-ketocholesterol are formed by oxidative processes in low-density lipoproteins and in atherosclerotic lesions and contribute to the pathology of disease. The plasma membrane of cells is not a homogeneous mixture of lipids but contains sphingolipid- and cholesterol-rich microdomains (lipid rafts) (*60*−*62*). Lipid rafts include or exclude proteins in response to intra- and extracellular stimuli. This favors specific protein−lipid and protein−protein interactions that modulate the activity of signaling cascades. Sterol structure, composition, and concentration are determinants of the protein composition of isolated raft domains and the membrane dynamics that reflect the biological processes associated with rafts (*5*, *6*, *63*−*65*). Methods that deplete the plasma membrane of cholesterol have been widely used to demonstrate the involvement of rafts in many cellular processes. However, the effects of increased plasma membrane cholesterol and oxysterol content, which characterize cholesterol-loaded macrophage foam cells located in atherosclerotic lesions, have received little attention (*5*, *6*). The hydrophobicity of oxysterols confines them to membranes where their modulating effects on the structure and domain formation of the plasma membrane may be responsible for their numerous in vitro cell biological effects. Sterols can promote or disrupt ordered membrane domain formation according to their specific chemical structures (*1*−*4*, *50*, *65*). 7-Ketocholesterol and 25-hydroxycholesterol support the formation of ordered lipid domains (*2*, *4*, *50*). Although addition of a carbonyl group to cholesterol to form 7-ketocholesterol is a small change in the covalent structure, its polarity and location in the proximity of the 3β-OH group locate both of these polar moieties near the hydrocarbon−water interfacial region of loosely packed L_d phospholipid bilayers (*3*, *35*, *37*, *38*, *66*). This decreases the depth of 7-ketocholesterol membrane intercalation and limits its interaction with phospholipid acyl chain termini (*3*, *35*, *37*, *38*, *66*). Also, the carbonyl group provides another interfacial dipole that could modulate binding of amphipathic proteins to the surface (*39*). An additional aspect of the increased polarity of 7-ketocholesterol is that it spontaneously transfers between membranes more than 20 times faster than cholesterol (*34*, *41*). Using spectroscopic methods, we have compared the effects of cholesterol on the phase behavior and lipid−protein interactions of model lipid membranes with those of 7-ketocholesterol, a "model" oxysterol with numerous physiological effects.

The main difference in the structures and properties of bilayers containing cholesterol and 7-ketocholesterol must be attributed to the additional carbonyl group in 7-ketocholesterol. The carbonyl group is small and relatively nonpolar, and in the tightly packed L_o phase, both sterols are probably oriented similarly quasi-perpendicular to the membrane plane (Figure 10; *67*). In L_d phases, cholesterol more than 7-ketocholesterol orders the bilayer and reduces interfacial polarity (Figure 3B,D,F and Table 1) (*3*, *4*), a finding that is consistent with a previous model in which the carbonyl group

Table 2: Rates and Half-Times for the Solubilization of DMPC MLVs by ApoA-I

	DMPC	DMPC and cholesterol		DMPC and 7-ketocholesterol	
temperature (°C)	k_{DMPC} (s^{-1})[a] [$t_{1/2}$ (min)]	k_C (s^{-1}) [$t_{1/2}$ (min)]	k_C/k_{DMPC}	k_{KC} (s^{-1}) [$t_{1/2}$ (min)]	k_{KC}/k_{DMPC}
22.8 ($T < T_M$)	5.73×10^{-6} (2020)	9.27×10^{-4} (12.4)	160	5.93×10^{-4} (19.5)	100
24.2 ($T = T_M$)	6.98×10^{-4} (16.5)	1.93×10^{-3} (5.98)	2.3	1.11×10^{-3} (10.4)	1.6
26.2 ($T > T_M$)	3.12×10^{-5} (370)	3.00×10^{-4} (38.5)	9.7	1.11×10^{-4} (104)	3.6

[a] Rate constants k_{DMPC}, k_C, and k_{KC} are for DMPC, DMPC containing 10 mol % cholesterol, and DMPC containing 10 mol % 7-ketocholesterol, respectively. The ratios of the rate constants for cholesterol to DMPC (k_C/k_{DMPC}) and for 7-ketocholesterol to DMPC (k_{KC}/k_{DMPC}) were calculated to determine the fold enhancement in the rate.

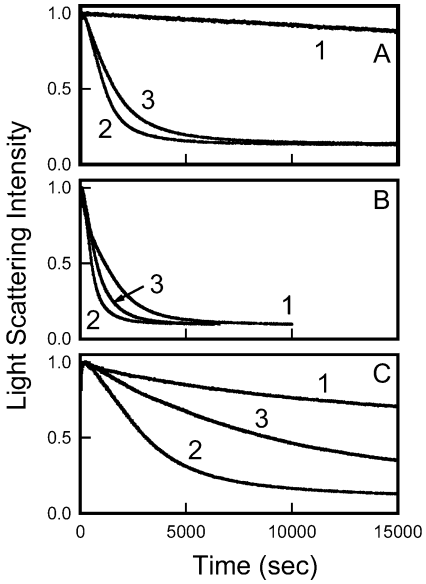

FIGURE 7: Kinetics of association of apoA-I with DMPC liposomes containing cholesterol and 7-ketocholesterol followed by changes in right angle light scattering as a function of time. The decrease in right angle light scattering is due to the conversion of the large multilamellar liposomes which scatter light to small rHDL which do not. The measurements were taken below the T_M (22.8 °C, A), at the T_M (24.2 °C, B), and above the T_M (26.2 °C, C) of DMPC. In panels A−C, the kinetic traces are for bilayers consisting of DMPC (curve 1), DMPC and 10 mol % cholesterol (curve 2), and DMPC and 10 mol % 7-ketocholesterol (curve 3). In panel A, the rate constants for DMPC, 10 mol % cholesterol, and 10 mol % 7-ketocholesterol were 5.73×10^{-6} s^{-1} ($t_{1/2} = 2020$ min), 9.27×10^{-4} s^{-1} ($t_{1/2} = 12.4$ min), and 5.93×10^{-4} s^{-1} ($t_{1/2} = 19.5$ min), respectively. In panel B, the rate constants for DMPC, 10 mol % cholesterol, and 10 mol % 7-ketocholesterol were 6.98×10^{-4} s^{-1} ($t_{1/2} = 16.5$ min), 1.93×10^{-3} s^{-1} ($t_{1/2} = 5.98$ min), and 1.11×10^{-3} s^{-1} ($t_{1/2} = 10.4$ min), respectively. In panel C, the rate constants for DMPC, 10 mol % cholesterol, and 10 mol % 7-ketocholesterol were 3.12×10^{-5} s^{-1} ($t_{1/2} = 370$ min), 3.00×10^{-4} s^{-1} ($t_{1/2} = 38.5$ min), and 1.11×10^{-4} s^{-1} ($t_{1/2} = 104$ min), respectively.

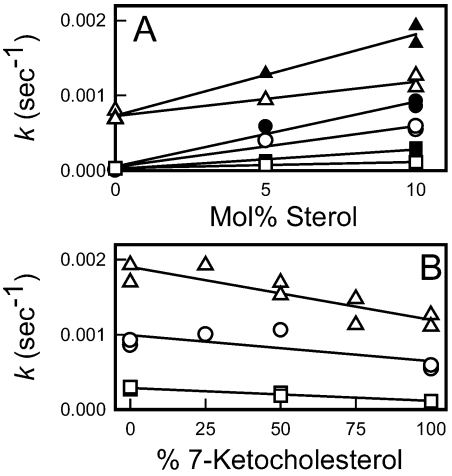

FIGURE 8: Kinetic traces for the changes of right angle light scattering for the association of apoA-I with DMPC liposomes analyzed as a pseudo-first-order process to obtain a rate constant (k). In panel A, the rate constants were determined as a function of cholesterol and 7-ketocholesterol concentration and temperature. The rate constants were determined for DMPC liposomes containing cholesterol (●, ■, and ▲) and 7-ketocholesterol (○, □, and △) where the measurements were taken at 22.8 (● and ○), 24.2 (▲ and △), and 26.2 °C (■ and □). In panel B, rate constant k was determined for DMPC liposomes containing mixtures of cholesterol and 7-ketocholesterol where the total amount of sterol was maintained at 10 mol %. The measurements were taken at 22.8 (○), 24.2 (△), and 26.2 °C (□).

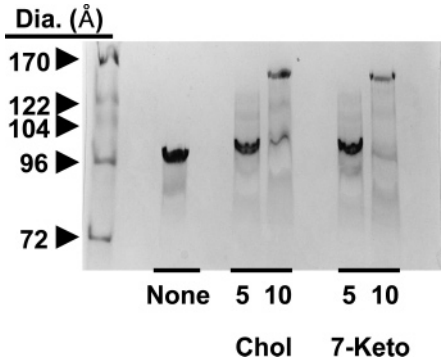

FIGURE 9: rHDL reaction products formed from the association of apoA-I with DMPC liposomes analyzed by nondenaturing polyacrylamide gel electrophoresis on 4 to 20% gradient gels. The samples that were analyzed were formed at 24.2 °C and contained no sterol, 5 and 10 mol % cholesterol (Chol), and 5 and 10 mol % 7-ketocholesterol (7-Keto). High-molecular weight standards of known diameter (Dia.) were also analyzed.

of 7-ketocholesterol (or the structurally similar 6-ketocholestanol) is oriented toward the aqueous phase by hydration, thereby tilting the sterol nucleus with respect to the bilayer plane so that it does not penetrate as far into the bilayer as cholesterol (Figure 10) (*3*, *35*, *37*, *38*, *66*). 6-Ketocholestanol extends ~6 Å less into the membrane bilayer than cholesterol does (*3*, *37*). The differential effects of the two sterols on L_o phase raft formation probably reflect differences in the driving forces that determine the orientation of 7-ketocholesterol in the bilayer: the increased van der Waals attractive interactions in the tightly packed L_o phase and hydrogen bonding of the carbonyl group with surface polar groups of phospholipids in the L_d phases.

Cholesterol and 7-ketocholesterol have similar effects on the properties of DMPC and DPPC MLVs. Both modulate the effects of the thermal transition on acyl chain order (Figure 1A,B). Below T_M, where there is a coexistence of gel and L_o phases, both sterols are equal in disrupting the

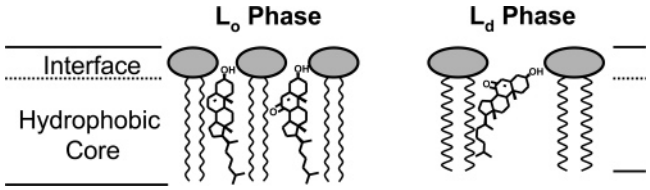

FIGURE 10: Proposed model for the biophysical properties of cholesterol and 7-ketocholesterol in which cholesterol and 7-ketocholesterol can form tightly packed L_o phases with phospholipids which have small interfacial surface areas, e.g., sphingomyelin and saturated phosphatidylcholines. In the less densely packed L_d bilayers of unsaturated phospholipids and phospholipids above their T_M, the carbonyl group of 7-ketocholesterol can become hydrated and hydrogen bond with interfacial polar groups, e.g., water, to relocate the sterol nucleus further from the bilayer center than cholesterol where the carbonyl group is located in the polar headgroup region. In phospholipid mixtures where L_o and L_d phases coexist, 7-ketocholesterol would have a stronger tendency than cholesterol to partition into the less densely packed L_d phase and would have a stronger tendency to destabilize membrane rafts.

acyl chain packing of gel phase lipids which indicates that they have a similar bilayer orientation (Figures 1A,B, 3A, and 4A). Equal behavior for cholesterol and 7-ketocholesterol was observed for the DRM measurements in DPPC bilayers which were also performed below T_M (Figure 5) (*4*). Above T_M, saturated PCs and SM in an L_d phase are more tightly packed than an unsaturated lipid such as DOPC (*68*). This also facilitates tighter phospholipid−sterol packing and greater acyl chain ordering upon the addition of sterol. Both sterols equally induce an L_d to L_o transition that is dose-dependent with respect to sterol content. Stronger sterol−phospholipid interactions were evident by the higher ΔP/mol % values for DPPC than for the DOPC/DPPC and DOPC/SM phospholipid mixtures at 55 °C (Table 1). Parallel measurements of GP show that the sterol-induced L_d to L_o conversion is associated with reduced interfacial hydration and polarity, an effect that is more profound with cholesterol than with 7-ketocholesterol (Figures 2A,B, 3B, and 4C and Table 1). The reduced level of hydration is a result of removing interfacial water by the tighter phospholipid−sterol packing that occurs in an L_o bilayer (*2*, *51*, *52*). Differences between the effect of the sterols on DMPC and DPPC bilayers may be attributed to the greater thickness of the DPPC bilayer, which permits its acyl chains to better fold under the cholesterol tail thereby permitting closer packing (*69*). This was apparent in the formation of DRMs, which form from mixtures of either cholesterol or 7-ketocholesterol with DPPC, whereas few or none form in mixtures of DMPC with cholesterol and 7-ketocholesterol (Figure 5). Low fluorescence polarization and GP (Figure 4) and no formation of DRMs (Figure 5) were observed in POPC and DOPC bilayers containing either sterol. These loosely packed L_d bilayers have been previously observed not to form L_o phases with added sterol (*4*, *70*, *71*).

The effects of cholesterol and 7-ketocholesterol in DOPC/DPPC and DOPC/SM mixed bilayers were more complex, nonlinear with respect to sterol concentration at 25 °C, but exhibit trends similar to those found in DPPC. It should be noted that the macroscopic behavior of these tertiary phospholipid/sterol mixtures is very different from that of binary phospholipid/sterol mixtures. The addition of cholesterol to DOPC/DPPC and DOPC/SM bilayers results in micrometer-scale liquid−liquid phase separation into microscopically visible domains that does not occur with cholesterol/DPPC bilayers (*57*, *59*). Thus, the nonlinear fluorescence responses to sterol concentration in tertiary mixtures reflect macroscopic behavior that does not occur in binary mixtures. According to DPH fluorescence polarization and GP, cholesterol increases bilayer order (Figure 1C,D) and reduces interfacial hydration more than 7-ketocholesterol (Figure 2C,D). These effects were dose-dependent at both 25 and 55 °C (Figure 3). Increasing the temperature from 25 to 55 °C causes coexisting L_d and L_o phases to coalesce into a single liquid phase (*57*−*59*) in which changes in GP and DPH fluorescence polarization are linear with respect to the sterol concentration (Figure 3). Thus, the effects of cholesterol on the properties of DOPC/SM and DOPC/DPPC bilayers were greater than those of 7-ketocholesterol (i.e., greater slopes), particularly for GP (Table 1). The decrease in acyl chain ordering and the smaller decrease in polarity indicate that 7-ketocholesterol penetrates less deeply into the bilayer and maintains the interfacial hydration. The linear correlation of DPH fluorescence polarization, GP, DRM formation, and fluorescence quenching with the mole percent of 7-ketocholesterol (Figures 4−6) indicates that each sterol exerts independent, additive effects on bilayer properties. Thus, none of our experiments support the reported (*35*) synergism between cholesterol and 7-ketocholesterol on the bilayer properties but suggest that sterol-specific differences in structure and properties determine domain formation.

Whereas cholesterol supported DRM formation by DOPC/DPPC and DOPC/SM bilayers, substitution of 7-ketocholesterol for cholesterol reduced the level of DRM formation to ∼50 and ∼95%, respectively, in DOPC/DPPC and DOPC/SM bilayers (Figure 5). The DOPC/DPPC results were similar to those of Wang et al. (*4*). The steady-state fluorescence measurements reflect the additive effects of the probes in different membrane domains. The greater amount of cholesterol-induced ordered lipid domains, which would have lower interfacial polarity, indicated by DRM correlates with the increase in GP for cholesterol in DOPC/DPPC and DOPC/SM bilayers (Figure 2C,D). Also, the nonlinear concentration dependence for GP in DOPC/SM/cholesterol bilayers correlates with the level of DRM formation, and the linear response for GP in DOPC/SM/7-ketocholesterol bilayers correlates with an absence of DRM formation (Figure 3D).

According to quenching studies, cholesterol and 7-ketocholesterol increase the level of ordered lipid domain formation in mixtures of 12SLPC/DPPC and 12SLPC/SM bilayers. At 37 °C, this effect is much greater with cholesterol than with 7-ketocholesterol and with DPPC than with SM (Figure 6). In SM-containing bilayers, the effects of the two sterols on domain formation were similar in the fluorescence quenching assay and by formation of DRMs. 7-Ketocholesterol decreased the extent of formation of DRMs in DOPC/SM bilayers and the extent of formation of nonquenched ordered lipid domains in 12SLPC/SM bilayers. Both sterols equally stabilized the formation of DPPC-rich domains in12SLPC/DPPC bilayers at 25 °C, whereas 7-ketocholesterol was ∼50% as effective at 37 °C. However, using a similar assay, Wang et al. (*4*) produced slightly different results, where cholesterol and 7-ketocholesterol were equal in forming DPPC-rich domains over the temperature range of ∼20−55 °C. Our results and those of Wang et al. (*4*)

indicate that cholesterol and 7-ketocholesterol both demonstrate favorable sterol−DPPC interactions that allow the formation of ordered lipid domains in DPPC and DPPC/fluid PC bilayers. However, this is not the case for SM. The different effects in DPPC and SM are probably not lipid class-specific. Porcine brain SM, which has a mixed acyl chain composition, mostly $C_{18:0}$ and $C_{24:1}{}^{\Delta}15cis$, exhibits a broad gel to liquid-crystalline phase transition between 20 and 45 °C (*51*) and is miscible with DOPC. On the other hand, DPPC has a sharp phase transition at 40.6 °C (*55*), and DPPC and DOPC display some solid−liquid immiscibility (Figures 1D and 2D) (*57*). Thus, differences can more likely be attributed to the distinctive phase transition properties of these two lipids rather than to one being a PC and the other being a sphingolipid (*57*, *72*). Thus, 7-ketocholesterol partitions between L_o and L_d phases according to the specific biophysical and chemical properties of the phospholipids that might occur within and without membrane rafts.

One consequence of different membrane domains is that there is a mismatch of properties at the interface where the two phases meet (*60*, *61*). In model membranes, domain boundaries appear (a) at the thermal phase transition temperature where gel and L_d phases coexist, (b) with the addition of cholesterol, which forms L_o phases that coexist with gel or L_d phases, and (c) between phospholipids with solid−liquid phase immiscibility. At domain boundaries, there is increased passive ion permeability (*73*−*77*), phospholipid flip-flop (*78*), phospholipase activity (*79*), and protein insertion (*42*−*44*, *80*). The differential effects of cholesterol and 7-ketocholesterol on domain formation could determine the structure of membranes in cells and their interactions with extracellular proteins, including solubilization of membranes by apoA-I (*5*, *6*, *45*−*47*).

There were large differences in the kinetics of apoA-I solubilization of cholesterol- and 7-ketocholesterol-containing DMPC MLVs with coexisting L_d and L_o domains (Figure 7C), which because of domain mismatch are separated by a boundary region (*60*, *61*). Insertion of monomeric apoA-I into the membrane defects created by the boundary region between coexisting lipid phases is the rate-limiting step in its solubilization of DMPC MLVs with and without cholesterol (*42*−*44*, *48*, *55*). When the ratio of absorbed apoA-I to lipid on the bilayer surface is sufficiently high, the bilayer is destabilized and a portion "bud off", as rHDL (*81*). Our studies clearly show that formation of an additional phase and the attendant phase boundaries affect lipid−protein association, i.e., solubilization of DMPC liposomes by apoA-I, which increases in the following order: gel < $L_d \ll$ gel and L_d phases (Table 2). In all cases, addition of sterol, which induces dose-dependent L_o phase formation, increases the rate, although this effect is smaller when $T = T_M$, where two phases coexist even in the absence of sterol. The smaller effect of sterol on the rates when $T = T_M$ may reflect closer packing at the interface between L_d and L_o phases than between gel and L_d phases. The greater effect of cholesterol, compared to that of 7-ketocholesterol, on the formation of L_o phases is reflected in its greater effect on the rate of DMPC solubilization by apoA-I (Figure 7).

The difference in the rate of apoA-I-mediated solubilization of cholesterol- and 7-ketocholesterol-containing DMPC bilayers was greatest for bilayers with coexisting L_d and L_o phases, which emulate cell membranes (Figure 7C and Table 2). One effect of cholesterol may be its localization to domain edges where it could reduce the number of unfavorable interactions between domains and allow better intermixing (*60*, *61*). The more amphiphilic 7-ketocholesterol should be even more effective in reducing the number of unfavorable domain−domain interactions, thus decreasing the amount and size of lipid packing defects and inhibiting the insertion of surface active proteins such as apolipoproteins. Also, cholesterol induces positive membrane curvature (membranes "bulge out") at the boundary between the L_d and L_o phases which may be important in various cellular membrane processes (e.g., secretory vesicle formation) (*65*). ABCA1 and other lipid flippases, which pump phospholipid from one leaflet of the bilayer to the other, deform membranes (i.e., induce curvature) by creating an imbalance in the number of phospholipid molecules between the two leaflets (*82*). The induction of positive membrane curvature by cholesterol at domain boundaries and by an imbalance of membrane phospholipid (e.g., created by ABCA1) could be a driving force for the budding off of vesicles and the formation of nascent HDL. The initial step in reverse cholesterol transport is apolipoprotein-mediated cellular cholesterol efflux, which can be triggered by the interaction of apoA-I with the ABCA1 transporter, specialized membrane domains formed by this transporter, or both (*47*). Incorporation of 7-ketocholesterol into macrophage plasma membrane rafts decreases the level of cellular binding of apoA-I and inhibits cholesterol efflux (*5*, *16*) and, in our model system, decreases the rate of insertion of apoA-I into phospholipid membrane interfaces.

Our studies indicate that (1) 7-ketocholesterol is less effective than cholesterol in forming phospholipid−sterol complexes and probably lipid−protein complexes that support raft formation and dynamics, (2) the carbonyl group is likely in the interfacial region of bilayers where it would increase the membrane dipole potential and alter the binding of amphipathic proteins, and (3) 7-ketocholesterol affects the number or properties of phase boundaries which determine some membrane−protein interactions. In vitro, 7-ketocholesterol induces many physiological responses that are considered pro-atherogenic such as induction of apoptosis, activation of signal transduction pathways in inflammation, and inhibition of reverse cholesterol transport. Incorporation of 7-ketocholesterol into plasma membrane lipid rafts may be the primary mechanism by which this sterol affects these many diverse processes (*5*, *6*, *83*).

REFERENCES

1. Xu, X., Bittman, R., Duportail, G., Heissler, D., Vilcheze, C., and London, E. (2001) Effect of the structure of natural sterols and sphingolipids on the formation of ordered sphingolipid/sterol domains (rafts). Comparison of cholesterol to plant, fungal, and disease-associated sterols and comparison of sphingomyelin, cerebrosides, and ceramide, *J. Biol. Chem. 276*, 33540−6.
2. Wenz, J. J., and Barrantes, F. J. (2003) Steroid structural requirements for stabilizing or disrupting lipid domains, *Biochemistry 42*, 14267−76.
3. Li, X. M., Momsen, M. M., Brockman, H. L., and Brown, R. E. (2003) Sterol structure and sphingomyelin acyl chain length modulate lateral packing elasticity and detergent solubility in model membranes, *Biophys. J. 85*, 3788−801.
4. Wang, J., Megha, and London, E. (2004) Relationship between sterol/steroid structure and participation in ordered lipid domains

(lipid rafts): Implications for lipid raft structure and function, *Biochemistry 43*, 1010−8.
5. Gaus, K., Kritharides, L., Schmitz, G., Boettcher, A., Drobnik, W., Langmann, T., Quinn, C. M., Death, A., Dean, R. T., and Jessup, W. (2004) Apolipoprotein A-1 interaction with plasma membrane lipid rafts controls cholesterol export from macrophages, *FASEB J. 18*, 574−6.
6. Berthier, A., Lemaire-Ewing, S., Prunet, C., Monier, S., Athias, A., Bessede, G., Pais de Barros, J. P., Laubriet, A., Gambert, P., Lizard, G., and Neel, D. (2004) Involvement of a calcium-dependent dephosphorylation of BAD associated with the localization of Trpc-1 within lipid rafts in 7-ketocholesterol-induced THP-1 cell apoptosis, *Cell Death Differ. 11*, 897−905.
7. Colles, S. M., Maxson, J. M., Carlson, S. G., and Chisolm, G. M. (2001) Oxidized LDL-induced injury and apoptosis in atherosclerosis. Potential roles for oxysterols, *Trends Cardiovasc. Med. 11*, 131−8.
8. Jessup, W., Wilson, P., Gaus, K., and Kritharides, L. (2002) Oxidized lipoproteins and macrophages, *Vasc. Pharmacol. 38*, 239−48.
9. Biasi, F., Leonarduzzi, G., Vizio, B., Zanetti, D., Sevanian, A., Sottero, B., Verde, V., Zingaro, B., Chiarpotto, E., and Poli, G. (2004) Oxysterol mixtures prevent proapoptotic effects of 7-ketocholesterol in macrophages: Implications for proatherogenic gene modulation, *FASEB J. 18*, 693−5.
10. Maor, I., Kaplan, M., Hayek, T., Vaya, J., Hoffman, A., and Aviram, M. (2000) Oxidized monocyte-derived macrophages in aortic atherosclerotic lesion from apolipoprotein E-deficient mice and from human carotid artery contain lipid peroxides and oxysterols, *Biochem. Biophys. Res. Commun. 269*, 775−80.
11. Myers, S. J., and Stanley, K. K. (1999) *Src* family kinase activation in glycosphingolipid-rich membrane domains of endothelial cells treated with oxidised low-density lipoprotein, *Atherosclerosis 143*, 389−97.
12. Bocher, V., Millatt, L. J., Fruchart, J. C., and Staels, B. (2002) Liver X receptors: New players in atherogenesis? *Curr. Opin. Lipidol. 14*, 137−43.
13. Bjorkhem, I., and Diczfalusy, U. (2002) Oxysterols: Friends, foes, or just fellow passengers? *Arterioscler. Thromb. Vasc. Biol. 22*, 734−42.
14. Rimner, A., Al Makdessi, S., Sweidan, H., Wischhusen, J., Rabenstein, B., Shatat, K., Mayer, P., and Spyridopoulos, I. (2005) Relevance and mechanism of oxysterol stereospecifity in coronary artery disease, *Free Radical Biol. Med. 38*, 535−44.
15. Garcia-Cruset, S., Carpenter, K. L., Guardiola, F., Stein, B. K., and Mitchinson, M. J. (2001) Oxysterol profiles of normal human arteries, fatty streaks and advanced lesions, *Free Radical Res. 35*, 31−41.
16. Gaus, K., Dean, R. T., Kritharides, L., and Jessup, W. (2001) Inhibition of cholesterol efflux by 7-ketocholesterol: Comparison between cells, plasma membrane vesicles, and liposomes as cholesterol donors, *Biochemistry 40*, 13002−14.
17. Escher, G., Krozowski, Z., Croft, K. D., and Sviridov, D. (2003) Expression of sterol 27-hydroxylase (CYP27A1) enhances cholesterol efflux, *J. Biol. Chem. 278*, 11015−9.
18. Gesquiere, L., Loreau, N., and Blache, D. (1997) Impaired cellular cholesterol efflux by oxysterol-enriched high-density lipoproteins, *Free Radical Biol. Med. 23*, 541−7.
19. Gelissen, I. C., Brown, A. J., Mander, E. L., Kritharides, L., Dean, R. T., and Jessup, W. (1996) Sterol efflux is impaired from macrophage foam cells selectively enriched with 7-ketocholesterol, *J. Biol. Chem. 271*, 17852−60.
20. Han, J., Nicholson, A. C., Zhou, X., Feng, J., Gotto, A. M., Jr., and Hajjar, D. P. (2001) Oxidized low-density lipoprotein decreases macrophage expression of scavenger receptor B-I, *J. Biol. Chem. 276*, 16567−72.
21. Cader, A. A., Steinberg, F. M., Mazzone, T., and Chait, A. (1997) Mechanisms of enhanced macrophage apoE secretion by oxidized LDL, *J. Lipid Res. 38*, 981−91.
22. Lange, Y., Ye, J., Rigney, M., and Steck, T. (2000) Cholesterol movement in Niemann-Pick type C cells and in cells treated with amphiphiles, *J. Biol. Chem. 275*, 17468−75.
23. Kritharides, L., Jessup, W., Mander, E. L., and Dean, R. T. (1995) Apolipoprotein A-I-mediated efflux of sterols from oxidized LDL-loaded macrophages, *Arterioscler. Thromb. Vasc. Biol. 15*, 276−89.
24. Girao, H., Catarino, S., and Pereira, P. (2004) 7-Ketocholesterol modulates intercellular communication through gap-junction in bovine lens epithelial cells, *Cell Commun. Signaling 2*, 2.
25. Millanvoye-Van Brussel, E., Topal, G., Brunet, A., Do Pham, T., Deckert, V., Rendu, F., and David-Dufilho, M. (2004) Lysophosphatidylcholine and 7-oxocholesterol modulate Ca^{2+} signals and inhibit the phosphorylation of endothelial NO synthase and cytosolic phospholipase A_2, *Biochem. J. 380*, 533−9.
26. Hayden, J. M., Brachova, L., Higgins, K., Obermiller, L., Sevanian, A., Khandrika, S., and Reaven, P. D. (2002) Induction of monocyte differentiation and foam cell formation in vitro by 7-ketocholesterol, *J. Lipid Res. 43*, 26−35.
27. Huang, R. F., Yaong, H. C., Chen, S. C., and Lu, Y. F. (2004) In vitro folate supplementation alleviates oxidative stress, mitochondria-associated death signalling and apoptosis induced by 7-ketocholesterol, *Br. J. Nutr. 92*, 887−94.
28. Pedruzzi, E., Guichard, C., Ollivier, V., Driss, F., Fay, M., Prunet, C., Marie, J. C., Pouzet, C., Samadi, M., Elbim, C., O'Dowd, Y., Bens, M., Vandewalle, A., Gougerot-Pocidalo, M. A., Lizard, G., and Ogier-Denis, E. (2004) NAD(P)H oxidase Nox-4 mediates 7-ketocholesterol-induced endoplasmic reticulum stress and apoptosis in human aortic smooth muscle cells, *Mol. Cell. Biol. 24*, 10703−17.
29. Martinet, W., De Bie, M., Schrijvers, D. M., De Meyer, G. R., Herman, A. G., and Kockx, M. M. (2004) 7-Ketocholesterol induces protein ubiquitination, myelin figure formation, and light chain 3 processing in vascular smooth muscle cells, *Arterioscler. Thromb. Vasc. Biol. 24*, 2296−301.
30. Seye, C. I., Knaapen, M. W., Daret, D., Desgranges, C., Herman, A. G., Kockx, M. M., and Bult, H. (2004) 7-Ketocholesterol induces reversible cytochrome *c* release in smooth muscle cells in absence of mitochondrial swelling, *Cardiovasc. Res. 64*, 144−53.
31. Rosenblat, M., and Aviram, M. (2002) Oxysterol-induced activation of macrophage NADPH-oxidase enhances cell-mediated oxidation of LDL in the atherosclerotic apolipoprotein E deficient mouse: Inhibitory role for vitamin E, *Atherosclerosis 160*, 69−80.
32. Lehto, M., and Olkkonen, V. M. (2003) The OSBP-related proteins: A novel protein family involved in vesicle transport, cellular lipid metabolism, and cell signaling, *Biochim. Biophys. Acta 1631*, 1−11.
33. Li, Q. T., and Das, N. P. (1994) Comparison of the effects of cholesterol and oxysterols on phospholipid bilayer microheterogeneity: A study of fluorescence lifetime distributions, *Arch. Biochem. Biophys. 315*, 473−8.
34. Theunissen, J. J., Jackson, R. L., Kempen, H. J., and Demel, R. A. (1986) Membrane properties of oxysterols. Interfacial orientation, influence on membrane permeability and redistribution between membranes, *Biochim. Biophys. Acta 860*, 66−74.
35. Rooney, M., Tamura-Lis, W., Lis, L. J., Yachnin, S., Kucuk, O., and Kauffman, J. W. (1986) The influence of oxygenated sterol compounds on dipalmitoylphosphatidylcholine bilayer structure and packing, *Chem. Phys. Lipids 41*, 81−92.
36. Verhagen, J. C., ter Braake, P., Teunissen, J., van Ginkel, G., and Sevanian, A. (1996) Physical effects of biologically formed cholesterol oxidation products on lipid membranes investigated with fluorescence depolarization spectroscopy and electron spin resonance, *J. Lipid Res. 37*, 1488−502.
37. Smondyrev, A. M., and Berkowitz, M. L. (2001) Effects of oxygenated sterol on phospholipid bilayer properties: A molecular dynamics simulation, *Chem. Phys. Lipids 112*, 31−9.
38. Phillips, J. E., Geng, Y. J., and Mason, R. P. (2001) 7-Ketocholesterol forms crystalline domains in model membranes and murine aortic smooth muscle cells, *Atherosclerosis 159*, 125−35.
39. Allende, D., Vidal, A., Simon, S. A., and McIntosh, T. J. (2003) Bilayer interfacial properties modulate the binding of amphipathic peptides, *Chem. Phys. Lipids 122*, 65−76.
40. Barenholz, Y. (2004) Sphingomyelin and cholesterol: From membrane biophysics and rafts to potential medical applications, *Subcell. Biochem. 37*, 167−215.
41. Kan, C. C., Yan, J., and Bittman, R. (1992) Rates of spontaneous exchange of synthetic radiolabeled sterols between lipid vesicles, *Biochemistry 31*, 1866−74.
42. Pownall, H. J., Massey, J. B., Kusserow, S. K., and Gotto, A. M., Jr. (1979) Kinetics of lipid−protein interactions: Effect of cholesterol on the association of human plasma high-density apolipoprotein A-I with L-α-dimyristoylphosphatidylcholine, *Biochemistry 18*, 574−9.
43. Pownall, H. J., Massey, J. B., Kusserow, S. K., and Gotto, A. M., Jr. (1978) Kinetics of lipid−protein interactions: Interaction of

apolipoprotein A-I from human plasma high-density lipoproteins with phosphatidylcholines, *Biochemistry 17*, 1183−8.
44. Pownall, H., Pao, Q., Hickson, D., Sparrow, J. T., Kusserow, S. K., and Massey, J. B. (1981) Kinetics and mechanism of association of human plasma apolipoproteins with dimyristoylphosphatidylcholine: Effect of protein structure and lipid clusters on reaction rates, *Biochemistry 20*, 6630−5.
45. Gillotte, K. L., Zaiou, M., Lund-Katz, S., Anantharamaiah, G. M., Holvoet, P., Dhoest, A., Palgunachari, M. N., Segrest, J. P., Weisgraber, K. H., Rothblat, G. H., and Phillips, M. C. (1999) Apolipoprotein-mediated plasma membrane microsolubilization. Role of lipid affinity and membrane penetration in the efflux of cellular cholesterol and phospholipid, *J. Biol. Chem. 274*, 2021−8.
46. Liu, L., Bortnick, A. E., Nickel, M., Dhanasekaran, P., Subbaiah, P. V., Lund-Katz, S., Rothblat, G. H., and Phillips, M. C. (2003) Effects of apolipoprotein A-I on ATP-binding cassette transporter A1-mediated efflux of macrophage phospholipid and cholesterol: Formation of nascent high-density lipoprotein particles, *J. Biol. Chem. 278*, 42976−84.
47. Yancey, P. G., Bortnick, A. E., Kellner-Weibel, G., de la Llera-Moya, M., Phillips, M. C., and Rothblat, G. H. (2003) Importance of different pathways of cellular cholesterol efflux, *Arterioscler. Thromb. Vasc. Biol. 23*, 712−9.
48. Massey, J. B., and Pownall, H. J. (1998) Interaction of α-tocopherol with model human high-density lipoproteins, *Biophys. J. 75*, 2923−31.
49. Massey, J. B., and Pownall, H. J. (1998) Surface properties of native human plasma lipoproteins and lipoprotein models, *Biophys. J. 74*, 869−78.
50. Xu, X., and London, E. (2000) The effect of sterol structure on membrane lipid domains reveals how cholesterol can induce lipid domain formation, *Biochemistry 39*, 843−9.
51. Massey, J. B. (2001) Interaction of ceramides with phosphatidylcholine, sphingomyelin and sphingomyelin/cholesterol bilayers, *Biochim. Biophys. Acta 1510*, 167−84.
52. Parasassi, T., Di Stefano, M., Loiero, M., Ravagnan, G., and Gratton, E. (1994) Cholesterol modifies water concentration and dynamics in phospholipid bilayers: A fluorescence study using Laurdan probe, *Biophys. J. 66*, 763−8.
53. London, E., and Brown, D. A. (2000) Insolubility of lipids in Triton X-100: Physical origin and relationship to sphingolipid/cholesterol membrane domains (rafts), *Biochim. Biophys. Acta 1508*, 182−95.
54. Schuck, S., Honsho, M., Ekroos, K., Shevchenko, A., and Simons, K. (2003) Resistance of cell membranes to different detergents, *Proc. Natl. Acad. Sci. U.S.A. 100*, 5795−800.
55. McKeone, B. J., Pownall, H. J., and Massey, J. B. (1986) Ether phosphatidylcholines: Comparison of miscibility with ester phosphatidylcholines and sphingomyelin, vesicle fusion, and association with apolipoprotein A-I, *Biochemistry 25*, 7711−6.
56. de Almeida, R. F., Fedorov, A., and Prieto, M. (2003) Sphingomyelin/ phosphatidylcholine/cholesterol phase diagram: Boundaries and composition of lipid rafts, *Biophys. J. 85*, 2406−16.
57. Veatch, S. L., and Keller, S. L. (2003) Separation of liquid phases in giant vesicles of ternary mixtures of phospholipids and cholesterol, *Biophys. J. 85*, 3074−83.
58. Scherfeld, D., Kahya, N., and Schwille, P. (2003) Lipid dynamics and domain formation in model membranes composed of ternary mixtures of unsaturated and saturated phosphatidylcholines and cholesterol, *Biophys. J. 85*, 3758−68.
59. Veatch, S. L., Polozov, I. V., Gawrisch, K., and Keller, S. L. (2004) Liquid domains in vesicles investigated by NMR and fluorescence microscopy, *Biophys. J. 86*, 2910−22.
60. Simons, K., and Vaz, W. L. (2004) Model systems, lipid rafts, and cell membranes, *Annu. Rev. Biophys. Biomol. Struct. 33*, 269−95.
61. Mukherjee, S., and Maxfield, F. R. (2004) Membrane domains, *Annu. Rev. Cell Dev. Biol. 20*, 839−66.
62. Pike, L. J. (2004) Lipid rafts: Heterogeneity on the high seas, *Biochem. J. 378*, 281−92.
63. Anderson, R. G., and Jacobson, K. (2002) A role for lipid shells in targeting proteins to caveolae, rafts, and other lipid domains, *Science 296*, 1821−5.
64. Keller, R. K., Arnold, T. P., and Fliesler, S. J. (2004) Formation of 7-dehydrocholesterol-containing membrane rafts in vitro and in vivo, with relevance to the Smith-Lemli-Opitz syndrome, *J. Lipid Res. 45*, 347−55.
65. Bacia, K., Schwille, P., and Kurzchalia, T. (2005) Sterol structure determines the separation of phases and the curvature of the liquid-ordered phase in model membranes, *Proc. Natl. Acad. Sci. U.S.A. 102*, 3272−7.
66. Simon, S. A., McIntosh, T. J., Magid, A. D., and Needham, D. (1992) Modulation of the interbilayer hydration pressure by the addition of dipoles at the hydrocarbon/water interface, *Biophys. J. 61*, 786−99.
67. Aussenac, F., Tavares, M., and Dufourc, E. J. (2003) Cholesterol dynamics in membranes of raft composition: A molecular point of view from ^{2}H and ^{31}P solid-state NMR, *Biochemistry 42*, 1383−90.
68. Nagle, J. F., and Tristram-Nagle, S. (2000) Structure of lipid bilayers, *Biochim. Biophys. Acta 1469*, 159−95.
69. Chiu, S. W., Jakobsson, E., Mashl, R. J., and Scott, H. L. (2002) Cholesterol-induced modifications in lipid bilayers: A simulation study, *Biophys. J. 83*, 1842−53.
70. Schroeder, R., London, E., and Brown, D. (1994) Interactions between saturated acyl chains confer detergent resistance on lipids and glycosylphosphatidylinositol (GPI)-anchored proteins: GPI-anchored proteins in liposomes and cells show similar behavior, *Proc. Natl. Acad. Sci. U.S.A. 91*, 12130−4.
71. Ahmed, S. N., Brown, D. A., and London, E. (1997) On the origin of sphingolipid/cholesterol-rich detergent-insoluble cell membranes: Physiological concentrations of cholesterol and sphingolipid induce formation of a detergent-insoluble, liquid-ordered lipid phase in model membranes, *Biochemistry 36*, 10944−53.
72. van Duyl, B. Y., Ganchev, D., Chupin, V., de Kruijff, B., and Killian, J. A. (2003) Sphingomyelin is much more effective than saturated phosphatidylcholine in excluding unsaturated phosphatidylcholine from domains formed with cholesterol, *FEBS Lett. 547*, 101−6.
73. Cruzeiro-Hansson, L., and Mouritsen, O. G. (1988) Passive ion permeability of lipid membranes modelled via lipid-domain interfacial area, *Biochim. Biophys. Acta 944*, 63−72.
74. Cruzeiro-Hansson, L., Ipsen, J. H., and Mouritsen, O. G. (1989) Intrinsic molecules in lipid membranes change the lipid-domain interfacial area: Cholesterol at domain interfaces, *Biochim. Biophys. Acta 979*, 166−76.
75. Corvera, E., Mouritsen, O. G., Singer, M. A., and Zuckermann, M. J. (1992) The permeability and the effect of acyl-chain length for phospholipid bilayers containing cholesterol: Theory and experiment, *Biochim. Biophys. Acta 1107*, 261−70.
76. Clerc, S. G., and Thompson, T. E. (1995) Permeability of dimyristoyl phosphatidylcholine/dipalmitoyl phosphatidylcholine bilayer membranes with coexisting gel and liquid-crystalline phases, *Biophys. J. 68*, 2333−41.
77. Xiang, T. X., and Anderson, B. D. (1998) Phase structures of binary lipid bilayers as revealed by permeability of small molecules, *Biochim. Biophys. Acta 1370*, 64−76.
78. John, K., Schreiber, S., Kubelt, J., Herrmann, A., and Muller, P. (2002) Transbilayer movement of phospholipids at the main phase transition of lipid membranes: Implications for rapid flip-flop in biological membranes, *Biophys. J. 83*, 3315−23.
79. Jorgensen, K., Davidsen, J., and Mouritsen, O. G. (2002) Biophysical mechanisms of phospholipase A_2 activation and their use in liposome-based drug delivery, *FEBS Lett. 531*, 23−7.
80. Barlic, A., Gutierrez-Aguirre, I., Caaveiro, J. M., Cruz, A., Ruiz-Arguello, M. B., Perez-Gil, J., and Gonzalez-Manas, J. M. (2004) Lipid phase coexistence favors membrane insertion of equinatoxin-II, a pore-forming toxin from *Actinia equine*, *J. Biol. Chem. 279*, 34209−16.
81. Segall, M. L., Dhanasekaran, P., Baldwin, F., Anantharamaiah, G. M., Weisgraber, K. H., Phillips, M. C., and Lund-Katz, S. (2002) Influence of apoE domain structure and polymorphism on the kinetics of phospholipid vesicle solubilization, *J. Lipid Res. 43*, 1688−700.
82. Graham, T. R. (2004) Flippases and vesicle-mediated protein transport, *Trends Cell Biol. 14*, 670−7.
83. Garcia, A., Cayla, X., Fleischer, A., Guergnon, J., Alvarez-Franco Canas, F., Rebollo, M. P., Roncal, F., and Rebollo, A. (2003) Rafts: A simple way to control apoptosis by subcellular redistribution, *Biochimie 85*, 727−31.

BI0506425